Dipeptidyl peptidase 8 and 9: specificity and molecular characterization compared to dipeptidyl peptidase IV

Jais R. Bjelke, Jesper Christensen, Per F. Nielsen, Sven Branner, Anders B. Kanstrup, Nicolai Wagtmann, Hanne B. Rasmussen

Biochemical Journal Immediate Publication. Published on 13 Feb 2006 as manuscript BJ20060079

Dipeptidyl peptidase 8 and 9 specificity and molecular characterization compared to dipeptidyl peptidase IV

Jais R. Bjelke[*], *Jesper Christensen*[§], *Per F. Nielsen*[¤], *Sven Branner*[¤], *Anders B. Kanstrup*[%], *Nicolai Wagtmann*[+], *and Hanne B. Rasmussen*[*]

[*]Protein Structure and Biophysics, [¤]Protein Science, [%]Medicinal Chemistry and [+]Cancer & Immunobiology, Novo Nordisk A/S, Novo Allé, 2880 Bagsvaerd, Denmark. [§]Biotech Research Innovation Center, Fruebjergvej, 2100 Copenhagen Ø, Denmark.

Correspondence should be addressed to H.B.R. *e-mail*: hbrm@novonordisk.com

Biochemical Journal Immediate Publication. Published on 13 Feb 2006 as manuscript BJ20060079

Abstract

Dipeptidyl peptidases 8 and 9 have been identified as gene members of the S9b family of dipeptidyl peptidases. Here we report the characterization of recombinant dipeptidyl peptidase 8 and 9 using the baculovirus expression system. We have found that only full-length variants of the two proteins can be expressed as active peptidases of 882 and 892 amino acids for dipeptidyl peptidase 8 and 9, respectively. We further show that the purified proteins are active dimers and that they show similar Michaelis-Menten kinetics and substrate specificity. Both cleave the peptide hormones glucagon-like peptide-1, glucagon-like peptide-2, neuropeptide Y and peptide YY with marked kinetic differences compared to dipeptidyl peptidase IV. Inhibition of dipeptidyl peptidase IV, dipeptidyl peptidase 8 and 9 using the well-known dipeptidyl peptidase IV inhibitor valine pyrrolidide resulted in similar Ki values, indicating that this inhibitor is nonselective for any of the three dipeptidyl peptidases.

Keywords

S9b family, dipeptidyl peptidase, glucagon-like peptide, neuropeptide Y, peptide YY, valine pyrrolidide.

Abbreviations

DPP: dipeptidyl peptidase. EST: expressed sequence tag. GLP: glucagon-like peptide. NPY: neuropeptide Y. pNA: p-nitroanilide. PYY: peptide YY. Sf9: *Spodoptera frugiperda* 9. ValPyr: valine pyrrolidide.

Introduction

The heterogenous S9b family of dipeptidyl peptidases (DPP) is a growing family of serine peptidases, which is characterized by the first identified member DPP-IV (alias CD26, EC 3.4.14.5) [1]. DPP-IV was first identified by Hopsu-Havu and Glenner as an enzyme possessing a glycylproline β-naphthylamidase activity and it was later shown that DPP-IV have a general ability to cleave prolyl and alanyl peptide bonds at the penultimate position from the N-terminus [2-6]. Initially, the observed specificity of DPP-IV was assumed to be unique, but other dipeptidyl peptidases and related peptidases with similar specificity have been identified [7-8].

Lately two members of the S9b family DPP-8 and DPP-9 have been discovered and *in-silico* pinpointed to the two human chromosomes 15q22 and 19p13.3 [9-10]. The open reading frame of DPP-8 codes for 882 amino acids and has been reported to be a monomeric protein of approximately 100-kDa. Based on similarities with the tissue expression distribution of DPP-IV, hypothetical functions of DPP-8 in relation to T-cell activation and other immune functions have been suggested [9], but still no clear physiological roles have been reported. At least one DPP-8 splice variant of possible functional significance has been identified in the expressed sequence tag (EST) database (hEST id. 8047491), comprising a sequence, which from alignments with DPP-IV lacks part of the α/β hydrolase domain including the catalytic active residue Ser739 (see figure 1).

DPP-9 was identified *in-silico* by Abbott and colleagues (2000) and first cloned and expressed recombinantly by Olsen and Wagtmann (2002) [9-10]. They expressed an 863 amino acids cDNA variant giving an enzymatically inactive protein, which migrated with a molecular mass of approx. 98 kDa as determined from SDS-PAGE analysis [10]. No *in vivo* functions have been described for DPP-9 and an enzymatically active variant of a recombinant expressed variant of DPP-9 has been reported in two studies with an apparent

open reading frame of 863 amino acids [11-12]. Analysis of the up-stream cDNA sequence of DPP-9 has revealed another ATG translation start site than the one reported by any of the previous studies (see figure 1), thus prolonging the open reading frame to a total of 892 amino acids (Gene bank accession no. NM_139159).

A counter screen strategy designed for development of specific DPP-IV inhibitors, involving cloning, expression and characterization of the specificity profile of DPP-8, DPP-9 and DPP-IV, were undertaken. We used the baculovirus expression system for production of His-tagged constructs of both the splice-variant Δ657-757 and full-length 882 amino acid variants of DPP-8, and the 863 and 892 amino acid variants of DPP-9 (see figure 1). In contrast to previous reports [11-12], we found that only the full-length variants of both DPP-8 and DPP-9 were enzymatically active, and both were able to cleave the naturally occurring hormones GLP-1, GLP-2, NPY and PYY. Although the truncated form of DPP-9 could be expressed, no enzymatic activity could be detected using different putative substrates. Thus, these results indicate that only full-length expression of the paralogous genes of DPP-8 and DPP-9 produce enzymatically active proteins and that the mature proteins are able to cleave naturally-occurring peptides of the incretin and pancreatic hormone families.

Experimental section

Bioinformatics Searches of EST cDNA clones were performed using the NCBI EST database (Gene bank accession numbers for DPP-8 and DPP-9: AF221634 and NM_139159). The Vector NTI Suite 6.0 (InforMax Inc.) was used for sequence analysis, gene alignments and primer design. Analyses of the X-ray structure of recombinant human DPP-IV (PDB id 1N1M) were performed using Quanta and WebLab ViewerPro (Accelrys Inc.).

Cloning Full-length DPP-8_{882aa} and DPP-9_{892aa} DNA sequences were obtained using specific primers (obtained from TAG Copenhagen, see table 1) for PCR from purified HeLa cDNA as previously described [13] and the EST clone 8047491 (obtained from I.M.A.G.E. consortium Inc.) containing the splice variant sequence of DPP-8. Primers were designed from DPP-8 and DPP-9 cDNA sequences with flanking restriction sites for directional cloning. Obtained PCR products were cloned in a pCR2.1 vector (Invitrogen, San Diego, USA) and verified by full-length DNA sequencing. Correct clones were subcloned to pBacPAK-His3 transfer vector (Clonetech, San Diego, USA) for recombinant virus production. In this way, pBacPAC-His3 constructs of DPP-8_{882aa} and DPP-9_{892aa} and the splice variant of DPP-$8_{\Delta 657\text{-}757aa}$ were constructed using the multilinker site 94 bp from the start of the polyhedrin promoter. In this way, all N-terminal His-tag was constructed with the start sequence Met-Gly-His-His-His-His-His-His-Gly-Ser-Thr-Met-XXX. A C-terminal 6xHis-tagged construct of the 863 amino acids variant of DPP-9_{863aa} was obtained from a pCDM8-DPP9/His construct (kindly provided by Christina Olsen) as a *BamH*I/*EcoR*I digest and subcloned into baculovirus transfer vector pVL1393 in the multilinker site 179 bp from the start of the polyhedrin promoter (Invitrogen, San Diego, USA).

Recombinant baculovirus and expression Recombinant baculovirus was produced using derived *Autographa californica* nuclear polyhedrosis virus DNA and the baculovirus transfer vector constructs as described previously [13]. In short, purified transfer vectors with

recombinant inserts were mixed with purified virus DNA and transfected in *Spodoptera frugiperda* 9 (Sf9) cells using Lipofectin (GIBCO/BRL). Virus was amplified for production of high titer stocks using Sf9 cells. Intracellular expression of recombinant DPP-8 and DPP-9 was performed in large cell dishes (25 x 25 cm, Nunc, Roskilde, Denmark) using High5 insect cells. Typically, expressions of 10^9 – 10^{11} cells were used per batch. All insect cells were grown in Grace Insect medium supplemented with 0 – 10 % FCS, yeastolate, 20 mM L-glutamine and 50 μg/ml gentamycin in either tissue culture flasks or glass spinner bottles at 28ºC.

Protein purification Insect cells were harvested after 48 hours of incubation by centrifugation at 400 g for 10 min., washed three times with PBS and resuspended in hypotonic buffer (25 mM Hepes pH 7.5, 5 mM KCl and 1.5 mM $MgCl_2$) for 10 min. Cells were lysed by 15-20 strokes in a dounce homogenizer, incubated for 20 min. and adjusted slowly to 0.4 M NaCl. Extracts were cleared by centrifugation at 20,000 – 30,000 g for 30 min., adjusted to 5 mM imidazole, filtered using 0.45 μm filter and applied directly to a TALON resin (BD Biosciences, San Jose, USA) column of different sizes depending on cell expression magnitude. Typically for larger expressions of more that 10^{10} cells approx. 1 ml resin was used, while expressions of less than 10^8 cells a 0.3 – 0.5 ml column was prepared. Column was equilibrated with 25 mM Hepes pH 7.5, 0.4 M NaCl and 5 mM imidazole (designated buffer A). The column was first washed with 10 volumes of buffer A and second with 10 volumes of 50 mM NaCl adjusted buffer A. Elution was performed using 25 mM Hepes pH 7.5, 50 mM NaCl and 100 mM imidazole. Subsequent ion-exchange purifications of the eluted fractions were performed using a MonoQ column (Amersham Biosciences, Uppsala, Sweden) on an Äkta Purifer low-pressure chromatographic apparatus (Amersham Biosciences, Uppsala, Sweden). A gradient of 0 – 0.5 M NaCl in a 50 mM Tris, pH 8 buffer

was used. The fractions were concentrated on Centriprep YM-10 and Centricon YM-10 filter devices (Millipore Corporation, Billerica, USA).

SDS-PAGE/Coomassie analyses were performed using 4-12% gradient NuPAGE® Bis-Tris Gels (Invitrogen, San Diego, USA) and GelCode Blue Stain Reagent (Pierce, Perbio Science UK Ltd., Cramlington, England).

Protein concentrations were determined spectrophotometric using UV280/254 nm absorbance and molar absorption coefficients of 186,920, 138,130 and 148,330 M^{-1} cm^{-1} for DPP-IV, DPP-8 and DPP-9, respectively.

Size exclusion chromatography Size exclusion experiments performed using a Superdex200 10/300 GL column (Amersham Biosciences, Uppsala, Sweden). A buffer composition of 100 mM NaCl and 50 mM Tris, pH 8 was used. Flow was 0.25 ml/min throughout.

Dynamic light scattering (DLS) DLS was performed on a DynaPro Dynamic Light Scattering Instrument (Protein Solutions, Lakewood, USA). All data were measured at room temperature and analyses were performed using the supplied software package Dynamics version 5.

Enzymatic activity assays Enzymatic activity was determined kinetically at 37°C in standard buffer containing 50 mM Tris pH 7.4, 150 mM NaCl, 0.1% Triton X-100. Different p-nitroanilide (pNA) substrates were used, including AlaAlaPro-pNA, SuccinateAla-pNA, ArgPro-pNA, AlaPro-pNA, ValAla-pNA, GlyPro-pNA, GlyGly-pNA, AlaPhe-pNA, AlaAla-pNA. 50 µl substrate + 50 µl enzyme were used at the double concentration of substrate and enzyme and released pNA was detected spectrophotometrically at 405 nm every 5 min. for a total of 30 min. in a kinetic SpectraMax 340 microplate reader (Global Medical Instrumentation, Inc., Minnesota, USA). Steady-state Michaelis–Menten kinetics were determined using 2-fold dilutions of the substrate and fitted directly to the Michaelis–Menten equation, $v = ([S] \times V) / ([S] + Km)$. Protein concentrations were optimized to give the best

absorbance readout during the 30 min. incubation and were 0.65, 13.5 and 15.5 nM for DPP-IV, DPP-8_{882aa} and DPP-9_{892aa}, respectively. A molar absorption coefficient of 8.8 mM^{-1} cm^{-1} at 410 nm was used for determination of pNA concentration. The liberated amount of product pNA during incubations was determined using a standard curve obtained at 410 nm for varying concentrations of a pNA stock solution in the SpectraMax 340 microtiter reader. Detection limits were between approx. 1 nM and 1.5 μM.

Inhibition kinetics was performed for all purified enzymes using the well-known competitive DPP-IV inhibitor ValPyr and the substrate GlyPro-pNA. IC50 determinations were performed from measured enzyme velocities at varying concentrations of inhibitor of 30.0, 10.0, 3.33, 1.11, 0.37 and 0.12 μM and a constant substrate concentration equal to the Km value for each of the enzymes, *i.e.* 0.2 mM DPP-IV, 0.3 mM DPP-8_{882aa} and 0.4 mM DPP-9_{892aa}. Using the relationship IC50 / Ki = 1 + [S] / Km, Ki values were derived from the IC50 determinations. At least three measurements were performed for all kinetic determinations.

Matrix-assisted laser desorption ionization time-of-flight mass spectroscopy (MALDI-TOF MS) analysis MALDI-TOF MS was performed on a Voyager RP MALDI-TOF instrument (Perseptive Biosystems Inc., Framingham, MA) equipped with a nitrogen laser (337 nm). The instrument was operated in linear mode with delayed extraction, and the accelerating voltage in the ion source was 25kV. Sample preparation was done as follows: 1 μl sample-solution (0.5-1.0 mg/ml) was mixed with 10 μl matrix-solution (α-cyano cinnamic acid dissolved in a 5:4:1 mixture of acetonitrile : water : 3 % TFA) and 1 μl was deposited on the sample plate (Standard stainless steel) and allowed to dry. Calibration was performed using external peptide standards resulting in a mass accuracy of 0.1% in the relevant mass area.

MALDI-TOF MS was used for analysis of enzymatic digestion of proteins by trypsin and semi-quantitative determination of cleavage rates by DPP-8_{882aa} and DPP-9_{892aa} of the

peptides GLP-1, GLP-2, NPY and PYY (all from Peninsula Laboratories Europe LTD., Merseyside, England). For determination of peptide cleavage rates, 1.0 μM peptide was incubated with 0.1 μM purified protein (*i.e.* 10x molar excess) final concentration in 50 μl at room temperature and in standard buffer (see Enzymatic activity assays). Samples were withdrawn at times 0, 20 min., 4, and 24 hours without adding any stopping additive. Relative ratios and *in vitro* halftimes ($t_{½}$) were estimated from ratios between the MS intensities of intact and cleaved peptides. Peptide sequences and molecular masses are listed:

GLP-1 (3298 Da): HAEGTFTSDVSSYLEGQAAKEFIAWLVKGR

GLP-2 (3766 Da): HADGSFSDEMNTILDNLAARDFINWLIQTKITD

NPY (4272 Da): YPSKPDNPGEDAPAEDLARYYSALRHYINLITRQRY

PYY (4310 Da): YPIKPEAPGEDASPEELNRYYASLRHYLNLVTRQRY

Results

Expression and purification of recombinant variants of DPP-8 and DPP-9 DPP-8_{882aa}, DPP-$8_{\Delta 657\text{-}757aa}$, DPP-$9_{863aa}$ and DPP-9_{892aa} were expressed either as N- or C-terminal His-tagged constructs (theoretical molecular masses of His-tagged constructs: DPP-8_{882aa}: 102 kDa (N-terminal His-tag). DPP-9_{863aa}: 99 kDa (C-terminal His-tag). DPP-9_{892aa}: 103 kDa (N-terminal His-tag)) using the baculovirus expression system and chromatographic purified using TALON resin as outlined in the experimental section. Only expression and purification of the DPP-8_{882aa} and DPP-9_{892aa} N-terminal His-tagged constructs produced enzymatic active proteins. From the TALON purification, expressions of DPP-8_{882aa} and DPP-9_{892aa} resulted in an increase of specific activities of 30x and 7x fold compared to cell lysates and yields of 19 % and 35 %, respectively. Table 2 shows the purification scheme of DPP-8_{882aa} and DPP-9_{892aa}.

SDS-PAGE/Coomassie analysis of the full-length DPP-8_{882aa} purification revealed a protein band of approx. 111 kDa as compared with M_w standards, and accounted for more than 90 % of the total fractionated protein (see supplemental figure 1). Dipeptidyl peptidase activity could be measured in the TALON fraction, but further ion-exchange purification was necessary for demonstration of co-migration between intensity of the individual protein fractions within the peak and activity levels. Following ion-exchange purification, the protein purity reached > 95 % as determined from SDS-PAGE analysis. Approximately 0.05 – 0.1 mg of pure protein could be obtained per 10^{10} High5 cells. A trypsin digest of the 111 kDa SDS-PAGE protein band demonstrated a clear MALDI-TOF MS fragmentation pattern corresponding to DPP-8_{882aa}. More than 60 % of the sequence was covered by the analysis (data not shown).

DPP-8_{882aa} was difficult to handle and showed a high degree of lability. 12 hours of incubation of DPP-8_{882aa} aliquots at room temperature reduced the specific activity by more

than 85 % compared to freshly thawed stocks. Addition of 10 % v/v glycerol before freezing preserved activity somehow, but otherwise no actions or formulation screening were performed to preserve activity other than maintaining stocks on an ice bath during handling and prior to assay incubations. Expression and purification of the splice variant of DPP-$8_{\Delta 657\text{-}757aa}$ produced no enzymatically active protein from the TALON elution (data not shown).

The two DPP-9 variants were expressed and purified as distinct proteins of similar molecular masses of approx. 95 kDa as determined from molecular mass standards (see supplemental figure 2). However, a very different heterogeneity could be observed for the two fractionated proteins as demonstrated from SDS-PAGE-Coomassie analysis. DPP-9_{892aa} was homogeneous and more than 95 % pure after the TALON fractionation, while DPP-9_{863aa} showed a heterogeneous band pattern as evaluated from the SDS-PAGE/Coomassie analyses, probably due to a poor folding ability and stability, resulting in not only a smaller amount of soluble protein, but also in incorrect folding. Activity levels co-migrated with the fractionated 95 kDa protein from the DPP-9_{892aa} expression, while no enzymatic activity could be detected from the fractions of the expression of the DPP-9_{863aa} variant (see supplemental figure 2). 0.5 – 1 mg of pure protein of DPP-9_{892aa} could be obtained for approx. 10^{10} High5 cells.

In-gel enzymatic digestion by trypsin of the 95 kDa bands of both the short and long DPP-9 construct verified that the proteins were DPP-9 as determined from MALDI-TOF MS analysis (see figure 2 for example of DPP-9_{892aa}).

DPP-9_{892aa} showed a much higher stability compared to DPP-8_{882aa}, since several freeze-thaws and prolonged incubations at room temperature only affected the enzymatic activity slightly. Temperature profiling showed that both DPP-8_{882aa} and DPP-9_{892aa} lost significant activity at and above 45°C incubation, while optimal activities for both of the two proteins were between 35 and 40°C incubation. This is a clear difference compared to the very stable DPP-

IV, which showed a stepwise activity increase from 25°C and up to 45 °C at which DPP-IV displayed 100% activity.

Quaternary structure analysis of DPP-8 and DPP-9 using dynamic light scattering and size exclusion chromatography The quaternary structures of DPP-8_{882aa} and DPP-9_{892aa} were analyzed and compared to DPP-IV which is known to be a catalytically active homodimer (see for example Rasmussen et al., 2003 [15]). DLS was used to measure the hydrodynamic radius of the purified proteins in solution. DPP-8_{882aa} and DPP-9_{892aa} displayed strong DLS signals corresponding to hydrodynamic radii of 6.8 and 5.9 nm with polydispersities of 18.1% and 16.2% (see supplementary figure 3). Likewise, DPP-IV displayed a monodisperse signal with a radius of 5.0 nm, polydispersity of 0.1 % (data not shown). The protein peaks of DPP-8_{882aa}, DPP-9_{892aa} and DPP-IV all corresponded to close to 100 % of total mass in solution when subtracting the solvent peak.

To further analyze the quaternary structure, size exclusion chromatography was performed for DPP-IV, DPP-8_{882aa} and DPP-$9_{892aa,}$ and compared to retention volumes of high molecular mass standards (see figure 3). All three proteins migrated with a retention volume of approx. 12 ml corresponding to molecular masses slightly above 200 kDa. Together, this indicates that both DPP-8 and DPP-9 are catalytically active homodimers in solution as DPP-IV.

Recombinant DPP-8 and DPP-9 show distinct Michaelis-Menten kinetics and specificity for cleavage of putative pNA substrate analogues Dipeptidyl peptidase activity could be demonstrated for DPP-8_{882aa} and DPP-9_{892aa} using the putative substrates GlyPro-pNA, AlaPro-pNA, ValAla-pNA and ArgPro-pNA (see table 3). No tri- or endopeptidase activities were observed (given incubation and assay conditions outlined in the experimental section) as determined using the peptide analogue AlaAlaPro-pNA and the full-length peptides GLP-1, GLP-2, NPY and PYY in a MALDI-TOF MS assay, which is similar to the one described by

Lambeir et al., (2001) [14]. DPP-8_{882aa} and DPP-9_{892aa} were unable to cleave GlyGly-pNA, AlaAla-pNA and AlaPhe-pNA under the given assay conditions.

Very similar Michaelis–Menten kinetic profiles of the different substrates could be demonstrated for DPP-8_{882aa} and DPP-9_{892aa} with K_m values between 70 – 1220 μM, which were similar to DPP-IV values of 50 – 670 μM (see table 3). k_{cat} for DPP-8_{882aa} and DPP-9_{892aa} were generally lower compared to DPP-IV giving equally lower catalytic capacities. For example did we observe for the ArgPro-pNA substrate 23x and 22x fold lower k_{cat} / K_m for DPP-8_{882aa} and DPP-9_{892aa} vs. DPP-IV, respectively. Using the substrates GlyPro-pNA and AlaPro-pNA, k_{cat} / K_m for DPP-8_{882aa} and DPP-9_{892aa} were in the order of 10^6 $M^{-1}s^{-1}$ for both enzymes making them very competent in terms of catalytic performance, but poorer compared to DPP-IV both for these two and all other substrates tested.

Kinetics and specificity of recombinant DPP-8 and DPP-9 The ability to cleave the naturally-occurring peptides GLP-1, GLP-2, NPY and PPY was tested *in vitro* using a MALDI-TOF MS based assay. From semi-empirical analyses of the distribution of peptide fragments, different kinetics could be observed depending on the peptide substrate used (see figure 4), but very similar when comparing rates between DPP-8_{882aa} and DPP-9_{892aa}, which generally were markedly lower compared to DPP-IV.

Both DPP-8_{882aa} and DPP-9_{892aa} could cleave two amino acids from the N-terminal of all four peptides and both showed a kinetic favoring of the following order $NPY_{YP\text{-}AA34}$ > $GLP\text{-}2_{HA\text{-}AA31}$ > $GLP\text{-}1_{HA\text{-}AA28}$ >> $PYY_{YP\text{-}AA34}$, which differed compared to DPP-IV which showed $NPY_{YP\text{-}AA34}$ ≈ $PYY_{YP\text{-}AA34}$ > $GLP\text{-}1_{HA\text{-}AA28}$ > $GLP\text{-}2_{HA\text{-}AA31}$. *In-vitro* $t_{½}$-values were determined from ratios between the MS intensities of intact and cleaved peptides (see table 4) corresponding to the following relative rates DPP-IV/DPP-8/DPP-9: 1/0.5/0.5 for NPY, 1/0.1/0.06 for GLP-2, 1/0.05/0.03 for GLP-1 and 1/0.002/0.002 for PPY. NPY was the full-length peptide substrate cleaved best among the four substrates tested, while cleavage of PYY

were the lowest for DPP-8 and DPP-9 and strikingly lower compared to DPP-IV, which cleaved this substrate at the highest rate equal to the cleavage rate of NPY. Both DPP-8 and DPP-9 showed lower substrate turnovers for all the full-length peptide substrates compared to DPP-IV and further a specificity difference could be observed. Only the first two N-terminal amino acids of GLP-1 were cleaved by DPP-8 and DPP-9 as opposed to DPP-IV, which cleaved sequentially two dipeptides from the N-terminal of GLP-1. This was in accordance with the inability to cleave GlyGly-pNA by DPP-8/-9, since the P2' residue is Gly.

Inhibition of DPP-IV, DPP-8 and DPP-9 with ValPyr We used the competitive DPP-IV inhibitor ValPyr for inhibition studies of DPP-IV, DPP-8 and DPP-9 as outlined in the experimental section. We found that DPP-IV, DPP-8 and DPP-9 showed a similar kind of inhibition, resulting in very similar Ki values (see table 5). Thus, the inhibitor ValPyr was equally potent and hereby non-selective for any of the three S9b family members DPP-IV, DPP-8 and DPP-9.

Discussion

We have characterized recombinant full-length variants of DPP-8 and DPP-9 as enzymes with similar kinetic, specificity and inhibition profiles, including the ability to cleave naturally-occurring peptides GLP-1, GLP-2, NPY and PYY *in vitro*. Expression of a Δ657-757 splice variant of DPP-8 and a short 863 amino acid variant of DPP-9 produced no enzymatically active proteins, and regarding the latter, this result concurred with previously published [10] and unpublished expression studies performed in our laboratories using both an *in-vitro* translation system and COS cells. Distinct activities were observed only for the full-length variants of 882 and 892 amino acids for DPP-8 and DPP-9, respectively. These results are opposed to published data of a recombinant expression construct of the short 863 amino acid variant of DPP-9 reported active [11-12]. None of the earlier studies showed any clear co-migration between the expressed DPP-9_{863aa} protein and the dipeptidyl peptidase activity observed. In one of the studies, activity estimations were based on mammalian cell transfection experiments, making contamination of endogenous activity of DPP-IV a possibility [12]. In our study, distinctive verifications of all the purified proteins using MALDI-TOF MS analysis of trypsin digests of the purified recombinant proteins were performed. These results indicate that DPP-9 only can be produced as an enzymatically active protein when expressed as a full-length 892 a.a. variant. The 3D structure of full-length DPP-9 is required for understanding the implications of the N-terminal. However, one cannot rule out the possibility that the placement of a His-tag can play a critical role for the missing activity of the short form of DPP-9_{863aa}. In this study, a His-tag was placed in the C-terminal of the short form, while in the studies reported by Qi and colleagues (2003) [11] and by Ajami and colleagues (2004) [12], the His-tag was placed in the N-terminal. In the construct of the long form of DPP-9_{892aa} the His-tag was placed in the N-terminal.

We have found that the DPP-8_{882aa} and DPP-9_{892aa} variants are dimers as determined using

size exclusion chromatography and dynamic light scattering. Thus, it appears that the general oligomeric structure of the S9b family members is a dimer configuration, since DPP-IV, FAPα and DPP-2 are dimers like DPP-8 and DPP-9 [16-17].

Assuming overall structural conservation between DPP-8, DPP-9 and DPP-IV, the published crystal structures of recombinant human DPP-IV can be used to deduce effects of the different variants [18-20]. DPP-IV is composed of an α/β-hydrolase and an 8-bladed β-propeller domain, in the interface of which the active site is located. The spliced exon Δ657-757 of DPP-8 comprises an essential part of the protein, since the active serine is located here according to sequence alignments and inspection of the X-ray structure of DPP-IV. When relating to the active site of DPP-IV[1], a distinct homology of 74% and 69 % identity can be observed between DPP-IV and DPP-8 and DPP-9 respectively, which is much higher than the relatively low overall identities of 20 % and 19 %, respectively. On the other hand, DPP-8 and DPP-9 are very homologous. They share an overall identity of 58 % and an identity of 92 % of essential active site residues as compared to DPP-IV. Remaining residues within the active site are possibly related to differences in substrate selectivity between DPP-8 and DPP-9 on one hand and DPP-IV on the other. In this context, it is notably that the well-known DPP-IV inhibitor ValPyr showed equipotency for all three enzymes, indicating that the inhibitor is non-selective contrary to the DPP-IV selectivity reported before DPP-8 and DPP-9 was made available [21]. Selectivity differences were also observed in the cleavage rates of four naturally-occurring peptides GLP-1, GLP-2, NPY and PYY, which generally were similar for DPP-8 and DPP-9 but higher for DPP-IV. NPY was the best substrate for all three enzymes and were cleaved with similar rates. DPP-IV cleaved PYY with a rate similar to NPY cleavage, which compared to DPP-8 and DPP-9 were approx. 500-fold higher. NPY and PYY have previously been reported as the best naturally-occurring substrates for DPP-IV

[1] Defined by a sphere of 8 Å radius from active site inhibitor ValPyr in DPP-IV and following pinpointing residues in alignment of DPP-8 and DPP-9.

[14,22]. Residue in the P1, P2 and P2' positions are the same in NPY and PYY, while the P1' residue differs being serine in NPY and isoleucine in PYY. Thus, a polar residue in the P1' position seem to be preferred for DPP-8 and DPP-9 relative to DPP-IV. Relating to the recently published DPP-IV crystal structure with a bound NPY analogue (pdb id. 1R9N), the S1' pocket appears flat and with no well defined contacts with the P1' serine [23] and the large active site cavity in itself explains the vast acceptance and high turnover of substrates. Indeed, DPP-8 and DPP-9 show difference in substrate selectivity of the P1 and P1' position compared to DPP-IV. Comparing the tested substrates there seem to be no requirements for the nature of a.a. in position P2 as both small and bulky side chains and non-polar and charged residues are tolerated. This is in analogy with what is found for DPP-IV. GLP-1 and GLP-2 were cleaved with similar rates by both DPP-8 and DPP-9, but approx. 10 – 30 fold lower compared to DPP-IV. Furthermore, we found that both DPP-8 and DPP-9 were unable to cleave substrates having glycine in the P1 position, which again is a distinct difference from the specificity of DPP-IV observed earlier [24] and by us. Given both the difference of substrate specificity between DPP-8, DPP-9 and DPP-IV and the suggested active site composition of DPP-8 and DPP-9, it is understandable that active site inhibitors with selectivity towards DPP-IV relative to DPP-8 and DPP-9 can be developed. These data suggest that S1 and S1' pockets might be explored for rational-drug design. *In vitro* selectivity data on a series of beta amino acid analogues has been reported by Kim and colleagues [25] and show that selectivity can be achieved. Animal data have indicated that inhibition of DPP-8 and DPP-9 produces a series of unwanted side-effects [26]. The importance for development of DPP-IV selective compounds for therapeutic use is hereby stressed.

DPP-8 and DPP-9 are examples of so-called DASH (DPP-IV activity and/or structure homologous) proteins, as they share sequence and possible structural homology as well as

functional activity with DPP-IV, and so might be associated with functions previously ascribed solely to DPP-IV. DPP-8 and DPP-9 have been reported to be intracellularly located, since no transmembrane domains or leader export signals for known cell secretion pathways have been identified in the sequence [8-10]. Thus, the *in vitro* observed proteolytic cleavage of the incretin hormones GLP-1 and GLP-2 by DPP-8 and DPP-9 is unlikely to be of relevance with respect to *in vivo* physiological functions, which DPP-IV has been attributed in the vascular system. An intracellular associated regulation of GLP-1 release from L-enterocytes is unlikely, since only intact GLP-1(7–37) has been shown to be secreted from L-enterocytes of the porcine ileum [27]. Regarding the pancreatic polypeptide family members PYY and NPY, it is interesting that these are regulated by enzymatic removal of the first dipeptide for production of selective Y receptor agonists, *e.g.* truncated PYY which is a highly selective Y2 receptor agonist [24,28]. However, the low cleavage rate observed for DPP-8 and DPP-9 speaks against a genuine physiologic role of the N-terminal processing of these pancreatic polypeptide hormones.

In conclusion, we have characterized different recombinant variants of DPP-8 and DPP-9 and found that only the full-length variants of 882 and 892 amino acids, respectively, were active enzymes, appearing to be homodimers in solution with very similar kinetic and substrate profiles. By analogy and comparison of the ability for DPP-8 and DPP-9 to cleave various substrates and naturally-occurring peptides of the incretin and pancreatic hormone family we have mapped requirements to a.a. nature in the proximal positions to the scissile bond and compared it to DPP-IV and conclude that development of DPP-IV selective therapeutic inhibitors relative to DPP-8 and DPP-9 is feasible.

Gene Bank ID. The sequence of the full-length 892 amino acid variant of DPP-9 has been deposited to the Gene bank.

Acknowledgement We thank Ulla Toftegaard and Dorte Mørch Gundesen for excellent technical assistance, and Dr. Richard Carr and Dr. Carolyn F. Deacon for excellent reviewing of the manuscript.

Reference list

1. Rawlings, N. D. and Barrett, A. J. (1999) MEROPS: the peptidase database. Nucleic Acids Res. **27,** 325-331
2. Hopsu-Havu, V. K. and Glenner, G. G. (1966) A new dipeptide naphthylamidase hydrolyzing glycyl-prolyl-beta-naphthylamide. Histochemie. **7,** 197-201
3. Kenny, A. J., Booth, A. G., George, S. G., Ingram, J., Kershaw, D., Wood, E. J., and Young, A. R. (1976) Dipeptidyl peptidase IV, a kidney brush-border serine peptidase. Biochem. J. **157,** 169-182
4. Kenny, A. J., Booth, A. G., Wood, E. J., and Young, A. R. (1976) Dipeptidyl peptidase IV, a kidney microvillus serine proteinase: evidence for its large subunit molecular weight and endopeptidase activity. Biochem. Soc. Trans. **4,** 347-348
5. Puschel, G., Mentlein, R., and Heymann, E. (1982) Isolation and characterization of dipeptidyl peptidase IV from human placenta. Eur. J Biochem. **126,** 359-365
6. Rawlings, N. D. and Barrett, A. J. (1993) Evolutionary families of peptidases.Biochem. J. **290 (Pt 1),** 205-218
7. Sedo, A. and Malik, R. (2001) Dipeptidyl peptidase IV-like molecules: homologous proteins or homologous activities? Biochim. Biophys. Acta **1550,** 107-116
8. Gorrell, M. D. (2005) Dipeptidyl peptidase IV and related enzymes in cell biology and liver disorders. Clin. Sci. (London) **108**, 277-292.
9. Abbott, C. A., Yu, D. M., Woollatt, E., Sutherland, G. R., McCaughan, G. W., and Gorrell, M. D. (2000) Cloning, expression and chromosomal localization of a novel human dipeptidyl peptidase (DPP) IV homolog, DPP8. Eur. J. Biochem. **267,** 6140-6150
10. Olsen, C. and Wagtmann, N. (2002) Identification and characterization of human DPP9, a novel homologue of dipeptidyl peptidase IV. Gene **299,** 185-193
11. Qi, S. Y., Riviere, P. J., Trojnar, J., Junien, J. L., and Akinsanya, K. O. (2003) Cloning and characterization of dipeptidyl peptidase 10, a new member of an emerging subgroup of serine proteases. Biochem. J. **373,** 179-189
12. Ajami, K., Abbott, C. A., McCaughan, G. W., and Gorrell, M. D. (2004) Dipeptidyl peptidase 9 has two forms, a broad tissue distribution, cytoplasmic localization and DPIV-like peptidase activity. Biochim. Biophys. Acta **1679,** 18-28
13. Christensen, J., Cotmore, S. F., and Tattersall, P. (1999) Two new members of the emerging KDWK family of combinatorial transcription modulators bind as a heterodimer to flexibly spaced PuCGPy half-sites. Mol. Cell Biol. **19,** 7741-7750
14. Lambeir, A. M., Durinx, C., Proost, P., Van Damme, J., Scharpe, S., and de Meester, I. (2001) Kinetic study of the processing by dipeptidyl-peptidase IV/CD26 of neuropeptides involved in pancreatic insulin secretion. FEBS Lett. **507,** 327-330
15. Rasmussen, H. B., Branner, S., Wiberg, F. C., and Wagtmann, N. (2003) Crystal structure of human dipeptidyl peptidase IV/CD26 in complex with a substrate analog. Nat. Struct. Biol. **10,** 19-25
16. Strop, P., Bankovich, A.J., Hansen, K.C., Garcia, K.C., Brunger, A.T. (2004) Structure of a human A-type potassium channel interacting protein DPPX, a member of the dipeptidyl aminopeptidase family. J Mol Biol. 2004 **343**,1055-1065
17. Aertgeerts, K., Levin, I., Shi, L., Snell, G.P., Jennings, A., Prasad, G.S., Zhang, Y., Kraus, M.L., Salakian, S., Sridhar, V., Wijnands, R., Tennant, M.G. (2005) Structural and kinetic analysis of the substrate specificity of human fibroblast activation protein alpha, J Biol Chem. **280**, 19441-19444
18. Hiramatsu, H., Kyono, K., Higashiyama, Y., Fukushima, C., Shima, H., Sugiyama, S., Inaka, K., Yamamoto, A., and Shimizu, R. (2003) The structure and function of human dipeptidyl peptidase IV, possessing a unique eight-bladed beta-propeller fold.

Biochem. Biophys. Res. Commun. **302,** 849-854

19. Thoma, R., Loffler, B., Stihle, M., Huber, W., Ruf, A., and Hennig, M. (2003) Structural basis of proline-specific exopeptidase activity as observed in human dipeptidyl peptidase-IV. Structure (Camb.) **11,** 947-959
20. Bjelke, J. R., Christensen, J., Branner, S., Wagtmann, N., Olsen, C., Kanstrup, A. B., and Rasmussen, H. B. (2004) Tyrosine 547 constitutes an essential part of the catalytic mechanism of dipeptidyl peptidase IV. J. Biol. Chem. **279,** 34691-34697
21. Deacon, C. F., Hughes, T. E., and Holst, J. J. (1998) Dipeptidyl peptidase IV inhibition potentiates the insulinotropic effect of glucagon-like peptide 1 in the anesthetized pig. Diabetes **47,** 764-769
22. Mentlein, R., Dahms, P., Grandt, D., and Kruger, R. (1993) Proteolytic processing of neuropeptide Y and peptide YY by dipeptidyl peptidase IV. Regul. Pept. **49,** 133-144
23. Aertgeerts K, Ye S., Tennant M.G., Kraus M.L., Rogers J., Sang B.C., Skene R.J., Webb D.R., Prasad G.S. (2004) Crystal structure of human dipeptidyl peptidase IV in complex with a decapeptide reveals details on substrate specificity and tetrahedral intermediate formation. Protein Sci. **13**, 412-421
24. de Meester, I., Korom, S., Van Damme, J., and Scharpe, S. (1999) CD26, let it cut or cut it down. Immunol. Today **20,** 367-375
25. Kim, D., Wang, L., Beconi, M., Eiermann, G. J., Fisher, M. H., He, H., Hickey, G. J., Kowalchick, J. E., Leiting, B., Lyons, K., Marsilio, F., McCann, M. E., Patel, R. A., Petrov, A., Scapin, G., Patel, S. B., Roy, R. S., Wu, J. K., Wyvratt, M. J., Zhang, B. B., Zhu, L., Thornberry, N. A., and Weber, A. E. (2005) (2R)-4-oxo-4-[3-(trifluoromethyl)-5,6-dihydro[1,2,4]triazolo[4,3-a]pyrazin-7(8H)-yl]-1-(2,4,5-trifluorophenyl)butan-2-amine: a potent, orally active dipeptidyl peptidase IV inhibitor for the treatment of type 2 diabetes. J. Med..Chem. **48**, 141-151
26. Edmondson, S. D., Mastracchio, A., Beconi, M., Colwell, L. F., Jr., Habulihaz, B., He, H., Kumar, S., Leiting, B., Lyons, K. A., Mao, A., Marsilio, F., Patel, R. A., Wu, J. K., Zhu, L., Thornberry, N. A., Weber, A. E., and Parmee, E. R. (2004) Potent and selective proline derived dipeptidyl peptidase IV inhibitors. Bioorg. Med..Chem. Lett. **14,** 5151-5155
27. Hansen, L., Deacon, C. F., Orskov, C., and Holst, J. J. (1999) Glucagon-like peptide-1-(7-36)amide is transformed to glucagon-like peptide-1-(9-36)amide by dipeptidyl peptidase IV in the capillaries supplying the L cells of the porcine intestine. Endocrinology **140,** 5356-5363
28. Grandt, D., Teyssen, S., Schimiczek, M., Reeve, J. R., Jr., Feth, F., Rascher, W., Hirche, H., Singer, M. V., Layer, P. and Goebell, H., (1992) Novel generation of hormone receptor specificity by amino terminal processing of peptide YY. Biochem. Biophys. Res. Commun. **186,** 1299-1306

Table 1: Primers used for cloning.

Primer name	Sequence
DPP-8_ forward_*Sal*I	5' *GTC GAC* CAT GGC AGC AGC AAT GGA AAC AGA A
DPP-8_revers_*Xba*I	5' *TCT AGA* TTA TTA TTA TATC ACT TTT AGA GCA GCA ATA
DPP-9_forward_1'ATG_*Sal*I	5' *GTC GAC* CAT GGC CAC CAC CGG GAC CCC AAC GG
DPP-9_revers#1_ *EcoR*I	5' *GAA TTC* TTA TTA TCA GAG GTA TTC CTG TAG AAA GTG C
DPP-9_forward_2'ATG_*Nde*I/*Sal*I	5' *CAT ATG GTC GAC* CAT GCG GAA GGT TAA GAA ACT GCG C
DPP-9_revers#2	5' CTC AGA GTA GAG GAG GGA GTT CTC TCG

Table 2: TALON purification.

	DPP-8_{882aa}	DPP-9_{892aa}
Cell lysate		
Protein amount (mg)	72	10
Total activity (µmole/min.)	358	524
Specific activity (µmole/min./mg)	5	52
Enrichment factor	1	1
%-Yield	100	100
TALON pool		
Protein amount (mg)	0.47	0.49
Total activity (µmole/min.)	69	184
Specific activity (µmole/min./mg)	148	376
Enrichment factor	30	7
%-Yield	19	35

Table 3: Kinetic parameters of putative substrates. Assays were performed with a buffer composition of 50 mM Tris pH 7.4, 150 mM NaCl, 0.1% Triton X-100 at 37 °C. Standard deviations of three experiments are given.

	Substrates	K_m (mM)	k_{cat} (s^{-1})	k_{cat}/K_m (s^{-1} M^{-1})
DPP-IV	GlyPro-pNA	0.20 ± 0.01	70.6 ± 0.3	430,500
	AlaPro-pNA	0.05 ± 0.01	38.0 ± 2.9	688,000
	ValAla-pNA	0.67 ± 0.09	57.0 ± 3.7	84,900
	ArgPro-pNA	0.06 ± 0.02	60.6 ± 12.8	898,400
DPP-8_{882aa}	GlyPro-pNA	0.33 ± 0.01	65.8 ± 0.2	199,300
	AlaPro-pNA	0.34 ± 0.10	65.0 ± 4.7	191,200
	ValAla-pNA	0.76 ± 0.08	1.5 ± 0.1	2,000
	ArgPro-pNA	0.07 ± 0.01	2.8 ± 0.2	40,900
DPP-9_{892aa}	GlyPro-pNA	0.37 ± 0.003	84.1 ± 1.1	227,100
	AlaPro-pNA	0.31 ± 0.13	90.0 ± 13.4	225,400
	ValAla-pNA	1.22 ± 0.13	2.5 ± 0.2	2,200
	ArgPro-pNA	0.06 ± 0.01	2.4 ± 0.2	41,200

Table 4: Relative $t_{½}$ values of peptide digests.		
	Peptides	$t_{½}$ (hrs)
DPP-IV	GLP-1	~ 0.2 (~ 1.2)*
	GLP-2	~ 0.4
	NPY	~ 0.1
	PYY	~ 0.1
DPP-8_{882aa}	GLP-1	~ 3.8
	GLP-2	~ 4.0
	NPY	~ 0.2
	PYY	~ 50
DPP-9_{892aa}	GLP-1	~ 6.1
	GLP-2	~ 6.7
	NPY	~ 0.2
	PYY	~ 48

*Value in parenthesis represents $t_{½}$ of degradation product GLP-1(11-36)

Table 5: Inhibition kinetics and selectivity of inhibitor ValPyr.					
Ki (µM)			**Selectivity**		
DPP-IV	***DPP-8_{882aa}***	***DPP-9_{892aa}***	***DPP-8_{882aa} / DPP-IV***	***DPP-9_{892aa} / DPP-IV***	***DPP-9_{892aa} / DPP-8_{882aa}***
0.64 ± 0.01	0.63 ± 0.02	0.78 ± 0.06	1	1	1

Figure legends

Figure 1: Protein sequence alignment of human DPP-IV, DPP-8 and DPP-9. Bold: 100% identity of at least two residues. Boxes: 100% identity throughout the residue. Important active site residues (see (14) and (17) for further details of the active site of DPP-IV) are indicated accordingly: (♦) Catalytic residues Tyr547, Ser630, Asp708 and H740. (▼) N-terminal coordinating residues Glu205 and Glu206. (●) Residues of the S1 pocket Tyr631, Val656, Trp659, Tyr662, Tyr666 and Val711. The prolonged open reading frame of DPP-9_{892aa} is indicated by an underline. The splice variant of DPP-$8_{\Delta 657\text{-}757aa}$ is indicated by a dashed underline.

Figure 2: In-gel digestion by trypsin of excised 95 kDa DPP-9_{892aa} bands were used for MALDI-TOF MS fragment analysis. MALDI-TOF MS fragment pattern of the digest is shown. More than 50% of the sequence was covered by the digest.

Figure 3: Chromatographic profiles of size exclusion analysis of DPP-IV, DPP-8_{882aa} and DPP-9_{892aa} on a Superdex200 column. Retention volumes of each protein analyzed are normalized to high-molecular mass standards (bottom) retention profile. Peaks were fractionated and analyzed for dipeptidyl peptidase activity. Indicated peaks showed dipeptidyl peptidase activity.

Figure 4: Fragmentation diagrams of MALDI-TOF MS analysis of GLP-1, GLP-2, NPY and PYY digests by DPP-8_{882aa} and DPP-9_{892aa}. Cleaved peptides are indicated by arrows. Very similar digest profiles could be obtained for DPP-8_{882aa} and DPP-9_{892aa}. Digested GLP-1 and -2 could be observed after 20 min. and were almost completely digested after 24 hours incubation. NPY digest products could be observed after 20 min. incubation and were digested to the end after less than 4 hours. Significant PYY digest products could first be

observed after approx. 4 hours and after 24 hours approx. 25 % were intact. See table 4 for estimated t½ values based on MALDI-TOF MS profiles.

Figure 1.

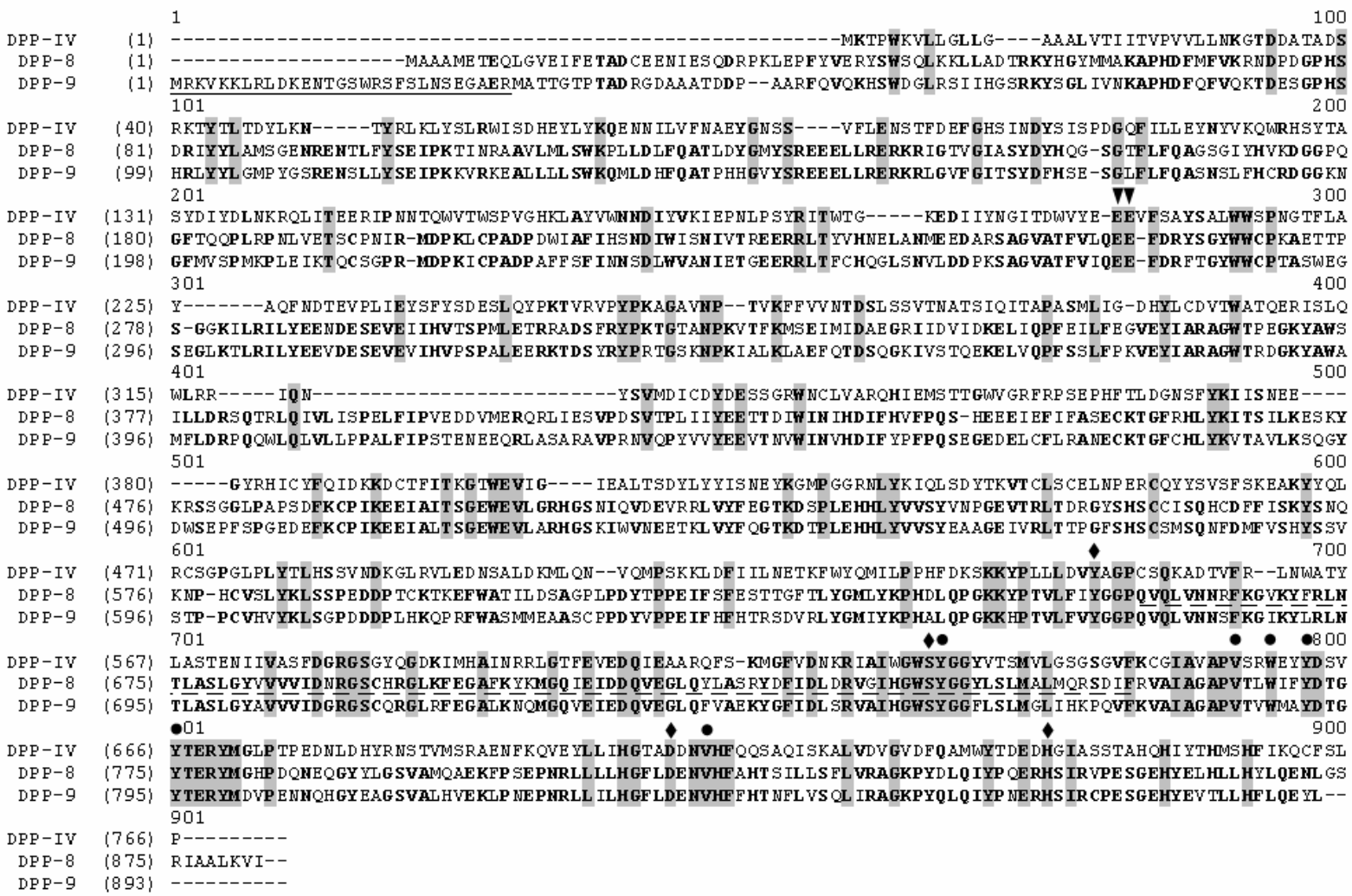

Biochemical Journal Immediate Publication. Published on 13 Feb 2006 as manuscript BJ20060079

Figure 2.

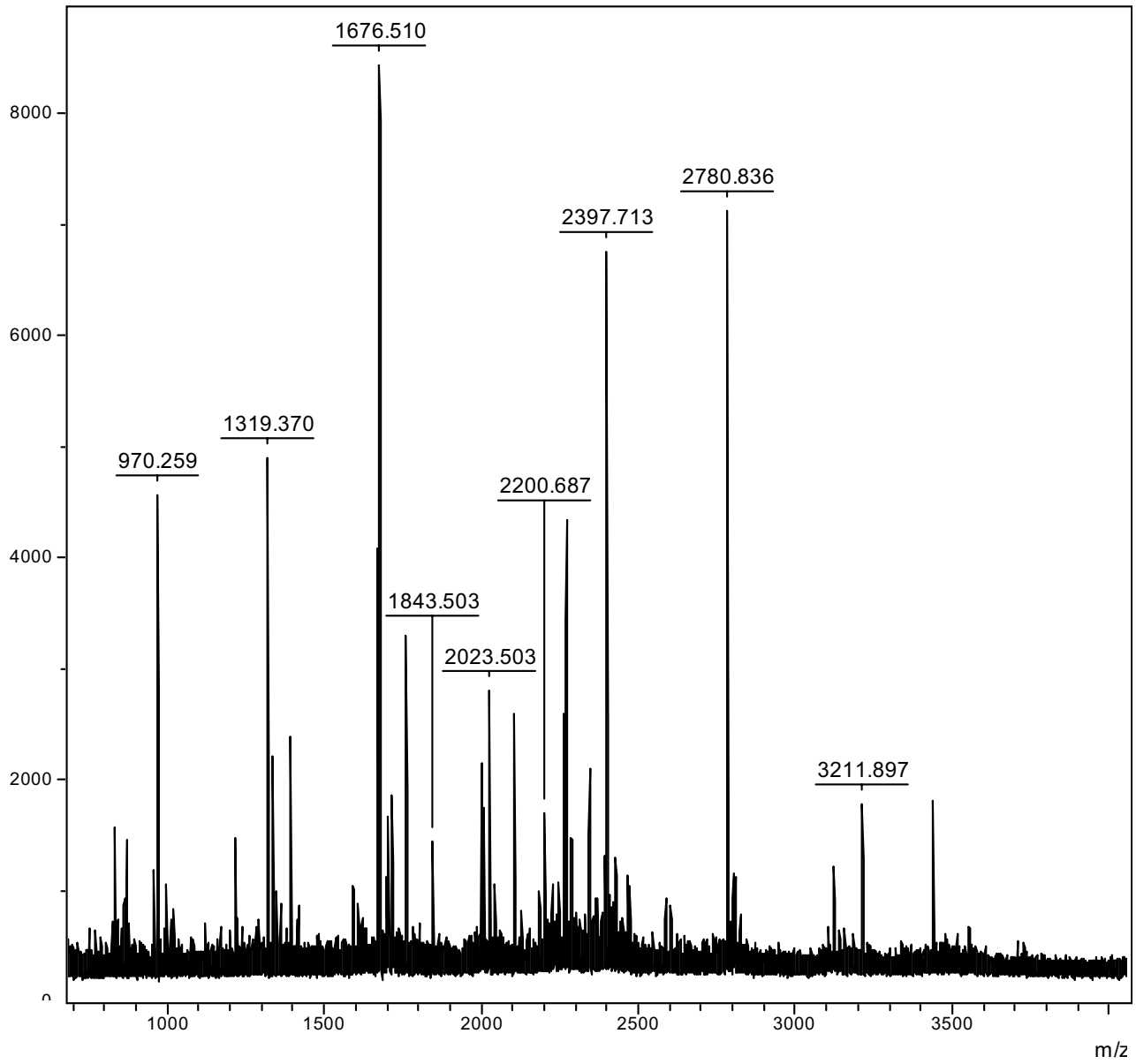

Bjelke et al.

Biochemical Journal Immediate Publication. Published on 13 Feb 2006 as manuscript BJ20060079

Figure 3.

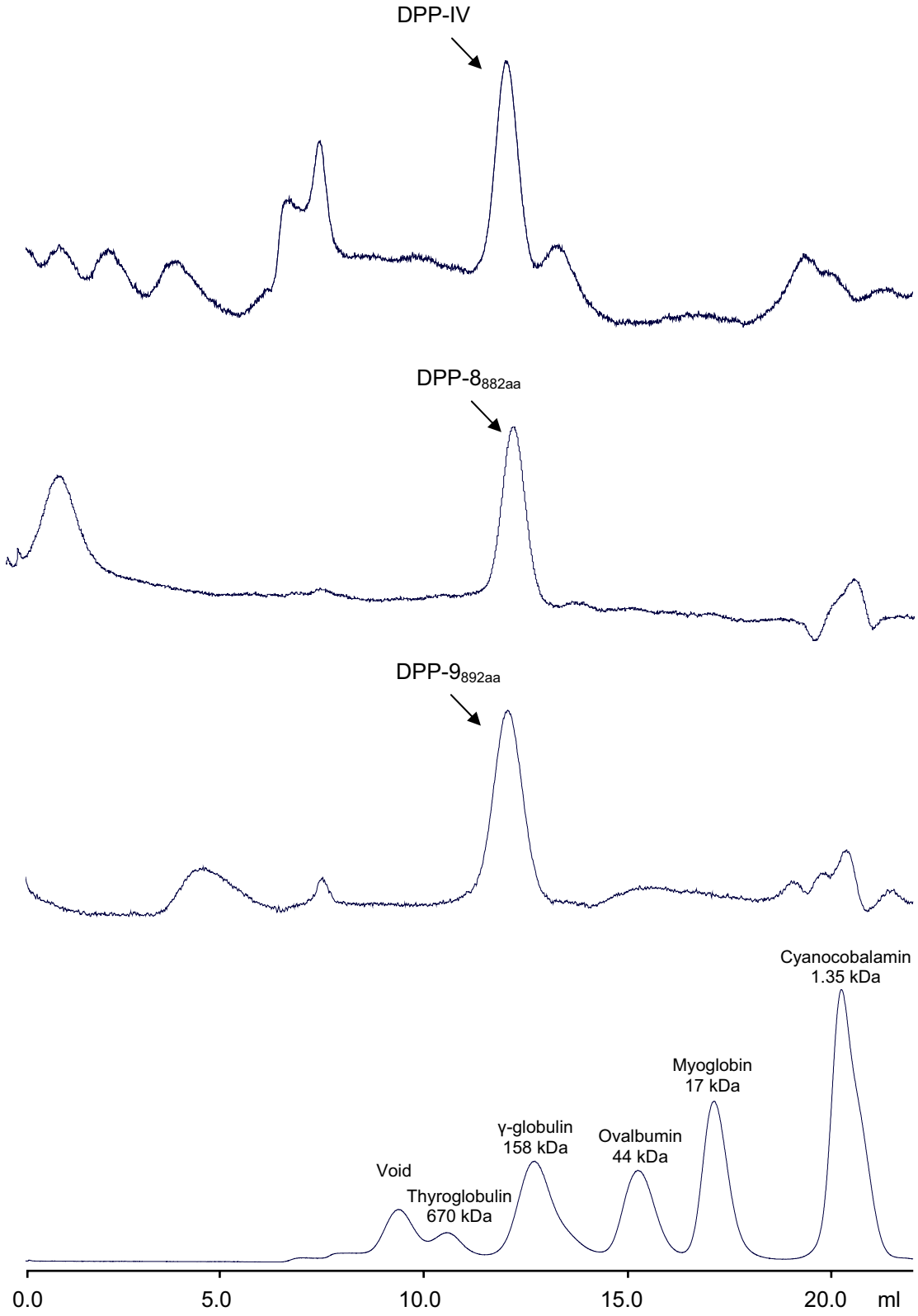

Bjelke et al.

Figure 4.

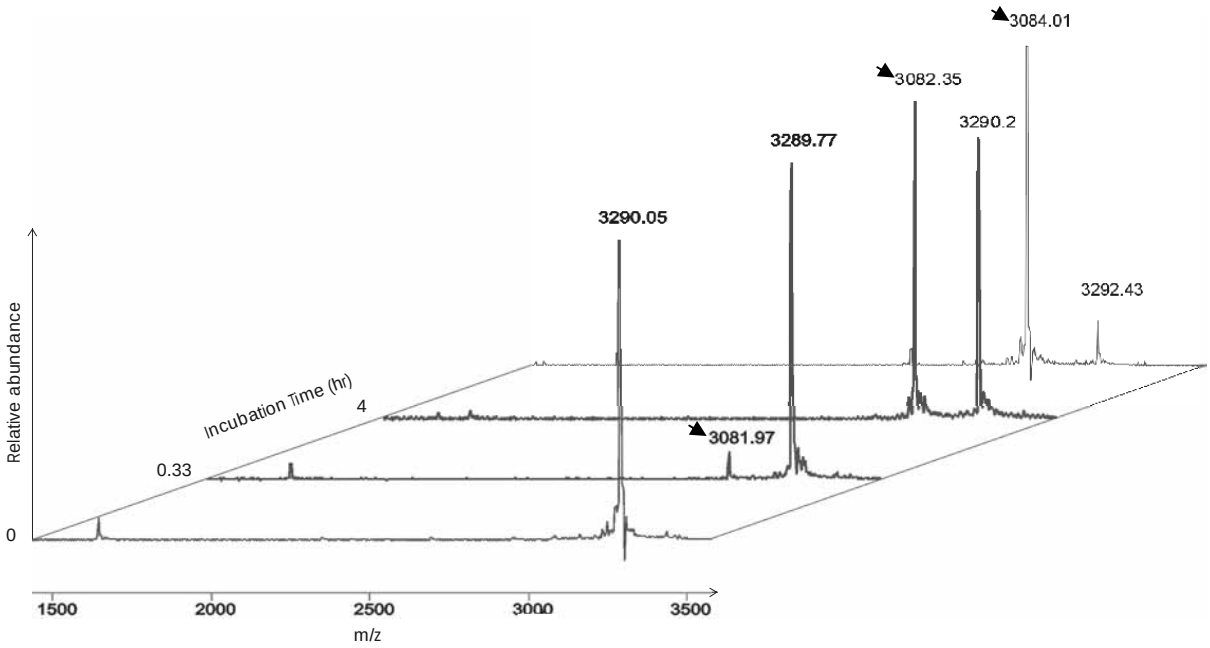

GLP-1 digest by DPP-8_{882aa}

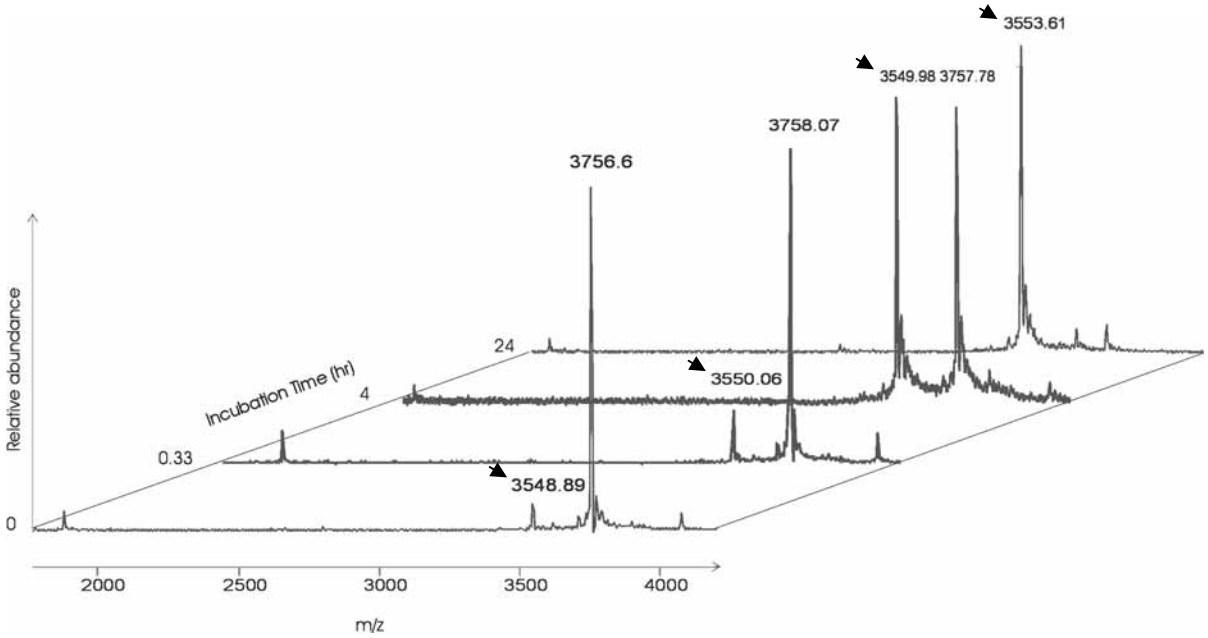

GLP-2 digest by DPP-8_{882aa}

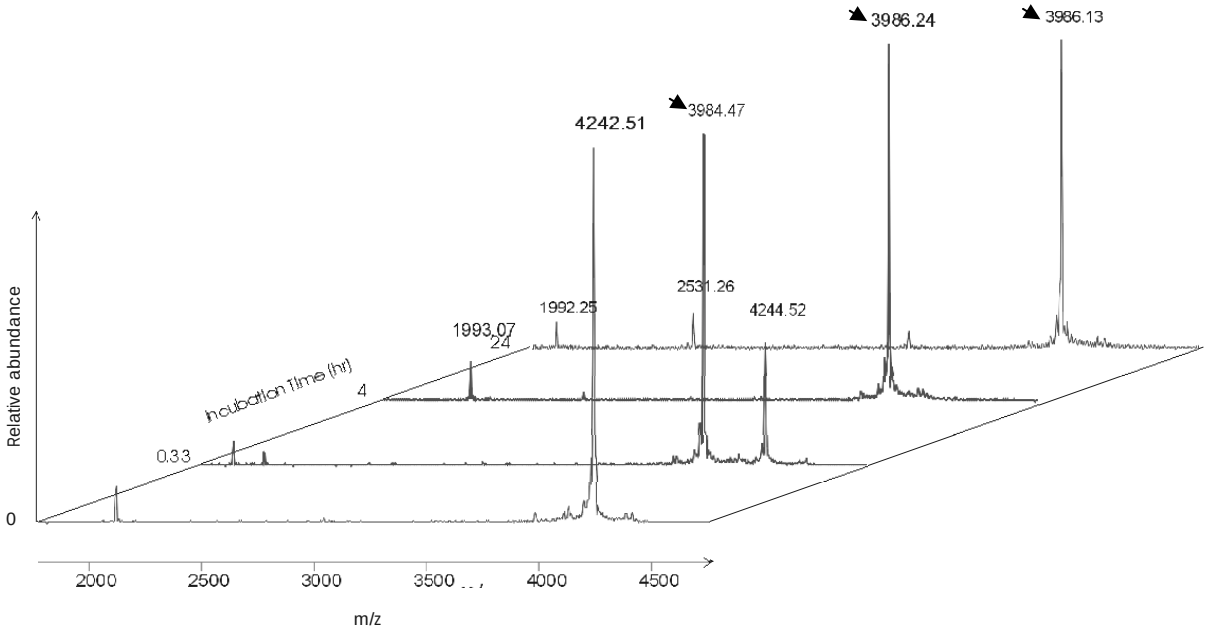

NPY digest by DPP-8_{882aa}

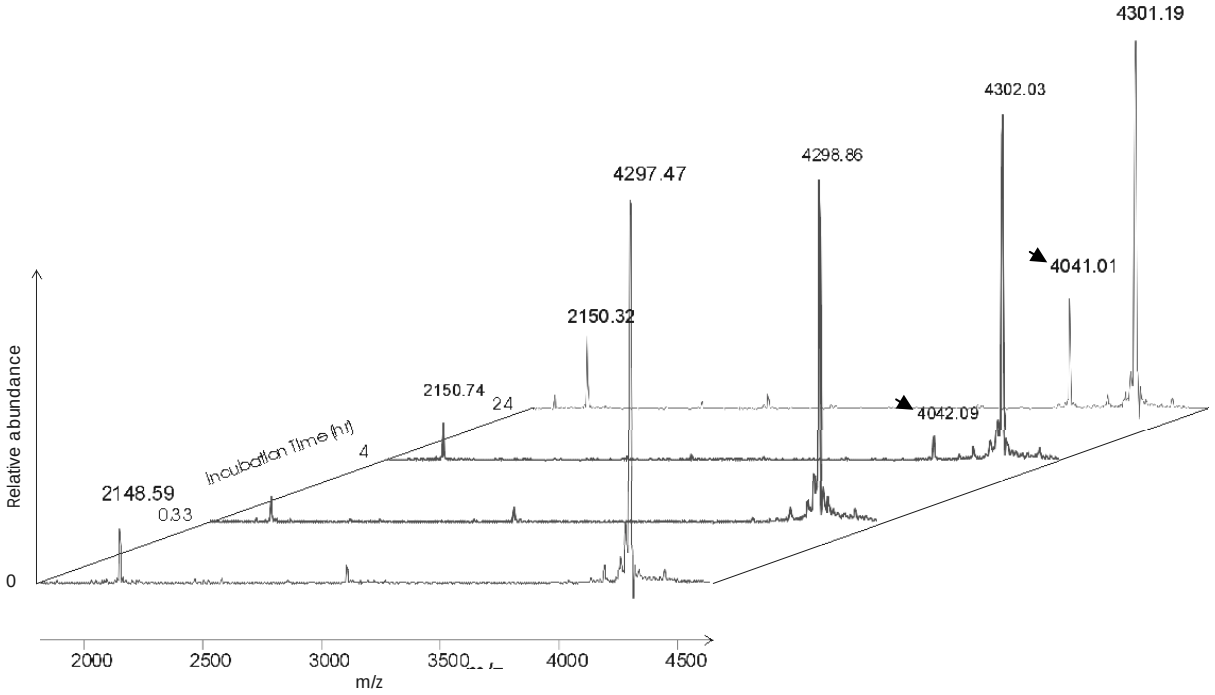

PYY digest by DPP-8_{882aa}

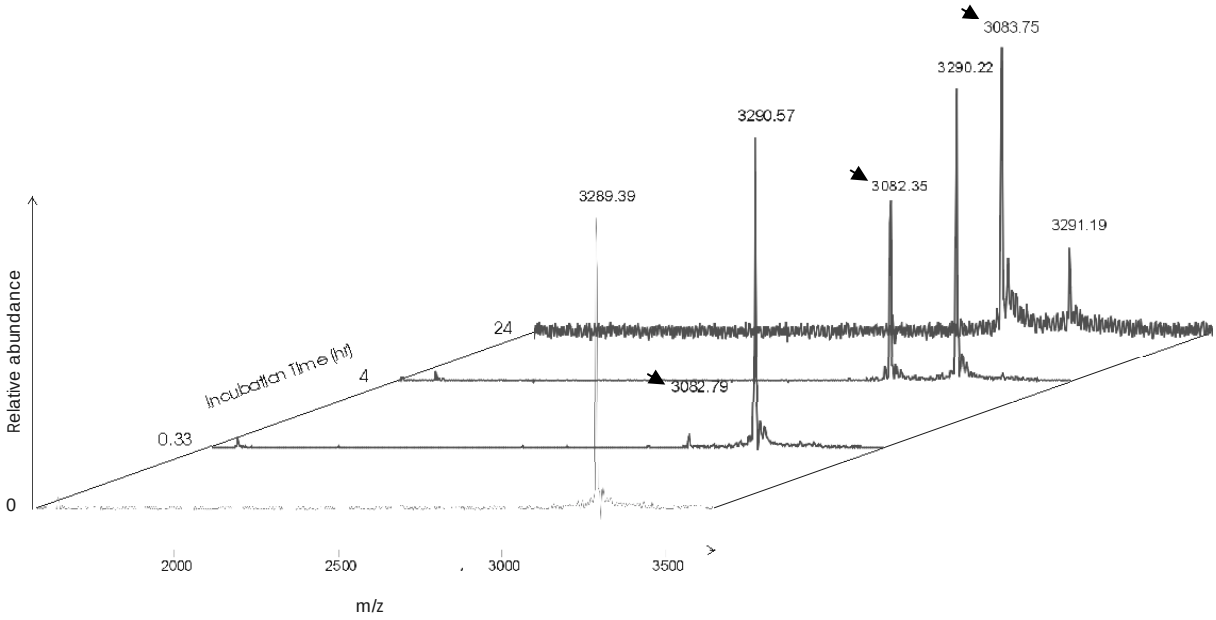

GLP-1 digest by DPP-9_{892aa}

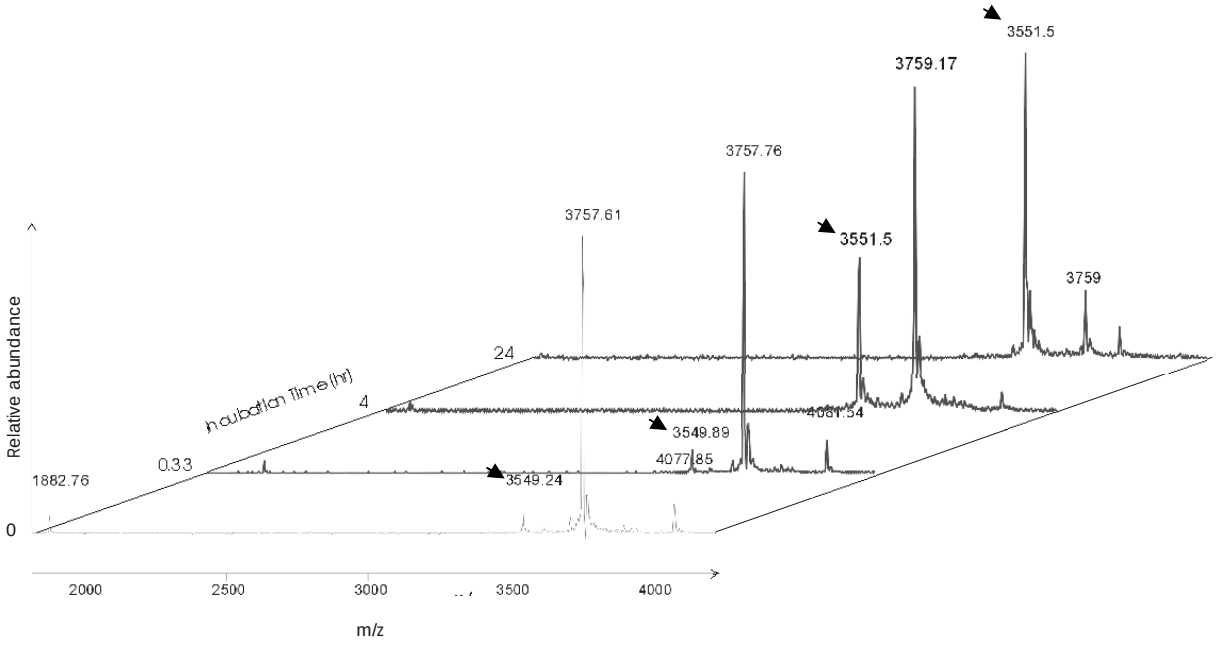

GLP-2 digest by DPP-9_{892aa}

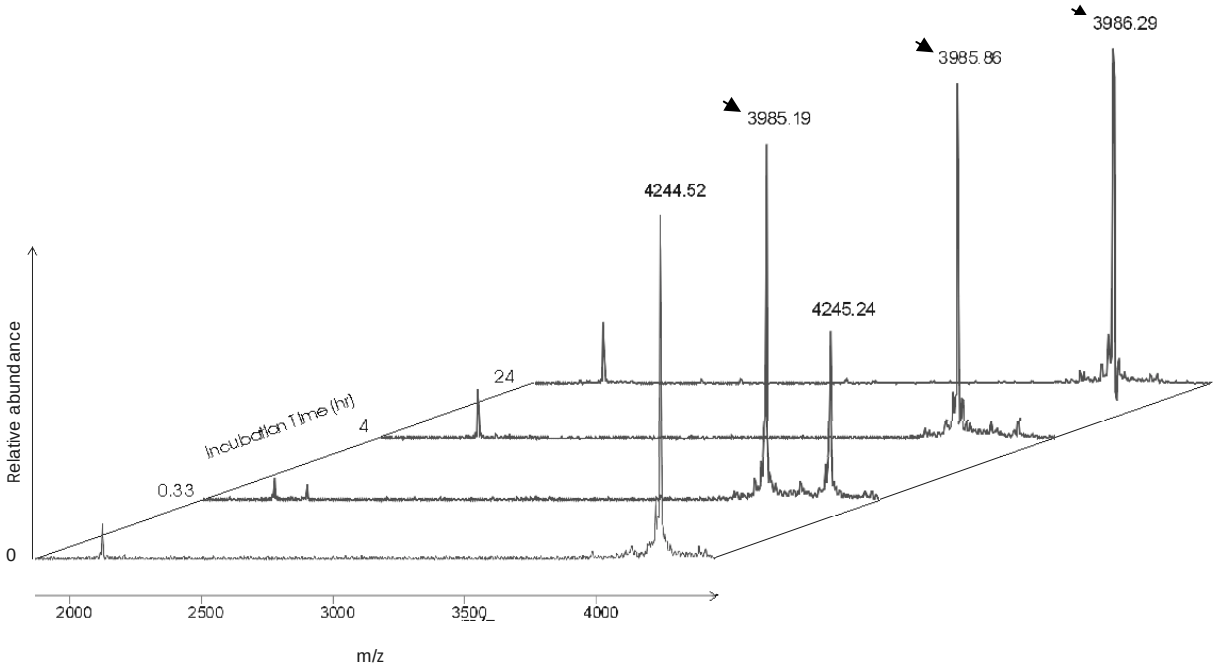

NPY digest by DPP-9_{892aa}

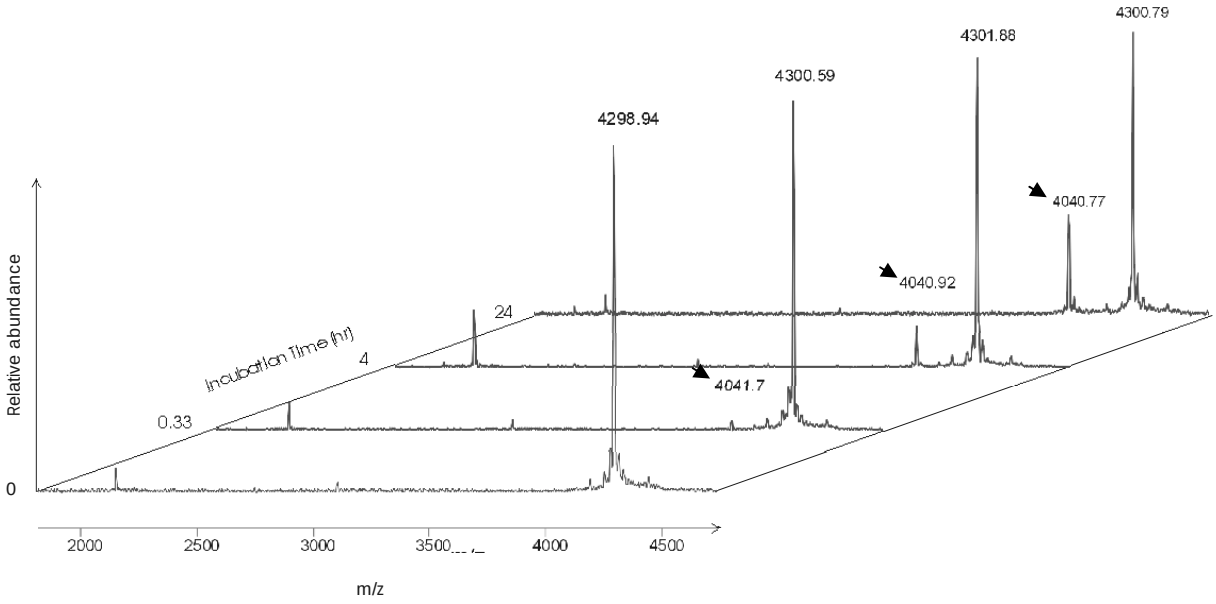

PYY digest by DPP-9_{892aa}